Bull. Mater. Sci., Vol. 22, No. 3, May 1999, pp. 353–362. © Indian Academy of Sciences.

Modeling of diffusion and oxidation in two dimensions during silicon device processing

P K SINGH and B K DAS*

Electronic Materials Division, National Physical Laboratory, New Delhi 110 012, India

Abstract. A process simulator named "2D-DIFFUSE" has been developed where the coupled diffusion equation of dopant impurity and point defects: interstitials and vacancies, has been solved numerically in two-dimension. The interaction of point defects has been modeled assuming quasi (i.e. local) equilibrium, $C_I C_V = C_I^* C_V^*$ and constant vacancy, $C_V = C_V^*$, conditions. Indeed, these two assumptions decouple the two point defects diffusion equations. The processes modeled in the present version of the simulator include pre-deposition, diffusion and oxidation. The simulator is quite successful at modeling each process individually as well as integrating various processes and models. The program has also been applied to the simulation of phenomena as the dopant diffusion under various ambients, oxidation enhanced and retarded diffusion, emitter push effect etc. Comparisons between simulation based on point defect parameters from various sources have been made.

Keywords. Diffusion; oxidation; process simulation; silicon device processing.

1. Introduction

Semiconductor industry no longer can afford to experiment in a trial-and-error manner due to involved complexity in VLSI device fabrication. The development of the present semiconductor devices with micron and submicron feature size relies heavily on the use of numerical simulation programs which indeed reduce time and cost in process and device development; offer yield optimization and provide insight into physical phenomenon involved in fabrication steps that are not accessible by experimental diagnostics (Wolf 1990).

The three classes of simulators i.e. process, device and circuit simulators are commonly used in actual semiconductor device design and optimize new device structures. The role of process simulators is in the prediction of process related behaviour to the device fabrication such as diffusion of dopant atoms, oxidation, ion implantation, etching, deposition of epitaxial layers of silicon and deposition of polysilicon and metal, etc and provides input for the other two class of simulators.

The activities in the area of simulation were started in the 1960s when the models for individual processes were developed (Atalla and Tannenbaum 1960; Lehovec and Slobodskoy 1961; Lindhard *et al* 1963; Grove *et al* 1964; Deal and Grove 1965; Hu and Schmidt 1968). The advent of SUPREM in the late seventies gave great impetus to the development of simulators and a large number of one-dimensional simulation programs, viz. SUPREM-II (Antoniadis and Dutton 1979), ICECREM (Ryssel *et al* 1980), SUPREM-III (Ho *et al* 1983), ASPREM (Sakamoto 1985), PREDICT (Fair 1988), PEPPER (Mulvaney *et al* 1989), etc followed. With time the device feature size was pushed from micron to sub-micron region and the need of 2D modeling became inevitable. The first 2-D process simulator "BIRD" was reported from Stanford University (Lee 1978), which was followed by simulators like SUPRA (Chin *et al* 1981), BICEPS (Penumalli 1983), ROMANS-II (Maldoado *et al* 1983), COMPOSITE (Lorenz *et al* 1985), SUPREM-IV (Kump and Dutton 1988), OPUS (Nishi *et al* 1989), FINDPRO (Rorris *et al* 1990), PREDICT-2 (Fair *et al* 1991), etc. Recently, more exhaustive and complete 2D process simulators: FEDSS (Borucki *et al* 1985), SAFEPRO (O'Brien *et al* 1985), IMPACT (Collard and Taniguchi 1986) based on finite element approach have also been developed because of the ease of tackling moving boundary.

Till recently Indian semiconductor industry was deprived of simulation tools because of the import restrictions on advanced versions of many simulators and non-availability of other proprietary codes of specific industries for their in-house use. It was realized that for the growth of our semiconductor industry, a strong knowledge base in this area is required. This led to the development of a one-dimensional process simulator named Silicon Technology Process Simulator, "1D-STEPS" in 1993 which is now commercially available (DoE 1993). In the continuity of this activity, two-dimensional process simulator "2D-DIFFUSE" was developed. "2D-DIFFUSE" is essentially for the simu-

*Author for correspondence

lation of two basic VLSI processing steps of diffusion and oxidation.

In this paper the salient features and the intricacies of impurity diffusion and oxidation for 2D features like bird's beak as derived from the two-dimensional process simulator "2D-DIFFUSE" have been discussed. For the exact modeling of diffusion phenomenon, the information about the point defects is vital as the substitutional dopant impurities diffuses either via interstitials or vacancies or both. This results in coupled diffusion equations involving dopant impurities and point defects. The program is based on the numerical solution of coupled diffusion of point defects: vacancies and interstitials and dopant impurities. The complications due to extremely stiff system of diffusion equations resulting due to many orders of magnitude difference in diffusion coefficients of the point defects and impurities have been addressed.

2. Basic point defects and impurity diffusion equation

The diffusion kinetics for point defects, interstitial and vacancies can usually be described well enough pragmatically by Fick's law with lumped recombination and generation terms as (Law 1990);

$$\frac{\partial (C_I - C_T)}{\partial t} = \nabla \cdot (D_I \nabla C_I) - K_R(C_I C_V - C_I^* C_V^*) + g_I , \tag{1}$$

$$\frac{\partial C_V}{\partial t} = \nabla \cdot (D_V \nabla C_V) - K_R(C_I C_V - C_I^* C_V^*). \tag{2}$$

The first terms on right hand side in (1) and (2) are conventional gradient driven diffusion with constant diffusion coefficients (D_I and D_V). The second terms model the recombination of interstitials and vacancies in terms of their local (C_I and C_V) and equilibrium (C_I^* and C_V^*) concentrations. The last term in (1) represents the interstitial generations during oxidation process. The trap kinetics (C_T) is coupled with the transient term and is given by following expression (Law 1990);

$$\frac{\partial C_T}{\partial t} = - K_T \left(C_T C_I - \frac{C_{ET}^*}{C_{TOT} - C_{ET}} C_I^* \, (C_{TOT} - C_T) \right), \tag{3}$$

where the subscript T, TOT and ET denotes effective, total and empty trap concentrations, respectively and the superscript star (*) denotes respective equilibrium values. K_R and K_T are recombination constants of the point defects inside bulk and traps, respectively.

The boundary conditions along the silicon–oxide interface for point defects are as follows (Law and Dutton 1988),

$$D_I \nabla C_I = K_I(C_I - C_I^*) + g_I , \tag{4}$$

$$D_V \nabla C_V = K_V(C_V - C_V^*) . \tag{5}$$

The same boundary conditions are valid at the back side of the wafer. Along the silicon surface covered with silicon nitride mask g_I is zero. The surface recombination constants, K_I and K_V provide a smooth transition between recombination velocities at oxidizing and inert interface and are functions of oxide growth rate (v_{ox}) and is defined by (Law 1990);

$$K_I = K_{I\max} \left(\frac{v_{ox}}{v_{ox}^0} \right)^{\alpha_I} + K_{I\min} , \tag{6}$$

$$K_V = K_{V\max} \left(\frac{v_{ox}}{v_{ox}^0} \right)^{\alpha_V} + K_{V\min} , \tag{7}$$

where v_{ox}^0 is initial oxide growth rate. α_I and α_V are decay parameters for the two-point defect species. The maximum ($K_{I\max}$ and $K_{V\max}$) and the minimum ($K_{I\min}$ and $K_{V\min}$) values of surface recombination velocities are derived at a growing and inert interfaces, respectively (Lin *et al* 1981).

The interstitial injection flux (generation) which is a function of position along the surface is given by (Hu 1974, 1985);

$$g_I = V_m \, \Theta \, v_{ox}^s \, \mathbf{n}, \tag{8}$$

where V_m and Θ are the lattice concentration of silicon ($= 5 \times 10^{22}$ cm^{-3}) and the percentage of silicon consumed, respectively and $\mathbf{n}$ is unit vector directed normal to oxide surface. The oxidation rate exponent s is assigned values from 0·5 to 1·0 (Hu 1983).

The diffusion kinetics for dopant impurities is also defined by Fick's law as (Wolf 1990; Singh and Das 1998);

$$\frac{\partial C_i}{\partial t} = \nabla \cdot \left[(D_i \nabla C_i) + \left(\frac{zq}{kT} \right) D_i C_i^{act} \mathcal{E} \right], \tag{9}$$

where C_i and C_i^{act} are the total and electrically active impurity concentration, respectively, D_i the diffusion coefficient of the diffusing impurity, z the charged state of the dopant (+ 1 for acceptors and − 1 for donors) and $\mathcal{E}$ the electric field. The symbols q, k and T have their usual meanings. The two terms on right hand side of (1) represents the classical gradient driven diffusion including non-constant diffusivity and the electro-static field driven flux respectively.

In the case of intrinsic diffusion when the dopant atoms are very dilute in a host lattice, the diffusion

coefficient is only a function of temperature and usually follows Arrhenius law. When dopant concentration exceeds intrinsic concentration, the diffusion coefficients no longer remain constant and are concentration dependent (Wolf 1990). This results in the non-linearity of (9).

The boundary conditions for dopant impurities are: (i) Along the silicon–oxide interface: (a) If the silicon surface is exposed to an impurity gas concentration

$$D_i \frac{\partial C_i}{\partial n} = h(C_i - C^{gas}). \quad (10)$$

(b) If the silicon surface is being oxidized (Seidl 1983);

$$D_i \frac{\partial C_i}{\partial n} = C_i \left(\frac{1}{\alpha m_{eq}} - 1 \right) v_{ox} \bar{n}. \quad (11)$$

(ii) Deep in the substrate: $C_i = 0$.

In the above equations α, m_{eq} and h are the volume expansion coefficient, the segregation coefficient and the evaporation coefficient, respectively. C^{gas} is the gas concentration.

The diffusion of impurities (9) and the point defects (1) and (2) are coupled by the following relation (Kump 1988; Kump and Dutton 1988),

$$D_i = D_i^* \left(f_{IA} \frac{C_I}{C_I^*} + (1 - f_{IA}) \frac{C_V}{C_V^*} \right), \quad (12)$$

where f_{IA} is the fractional interstitialcy factor.

3. Two-dimensional oxidation simulation

The two-dimensional oxidation effects are generally seen on non-planner surfaces such as trench structures, mask edges or polysilicon lines where the shape of the grown oxide develops as a "bird's beak". The formation of silicon dioxide by consuming silicon leads to the volume expansion and the grown oxide rearranges itself through viscous flow. The silicon–silicon dioxide interface moves continuously with time during processing adding complications in theoretical modelling. For the accurate simulation of oxidation process, a complete set of differential equations governing the oxide growth and viscous flow are to be solved numerically (Chin *et al* 1983a, b). To avoid complexity many process simulators viz. SUPRA (Chin *et al* 1981), SUPREM-IV (TSUPREM 1992) and OSIRIS (Guillemot *et al* 1987a, b), have used analytical expressions to simulate 2D oxidation. Our 2D oxidation is based on an analytical model after Guillemot *et al* (1987a).

When silicon nitride mask and pad oxide are thin, low stress is exerted on oxide and its thickness under (Z_1) and above (Z_2) the silicon surface is given as;

$$Z_1(y) = a_1\, erfc(b_1 y + c_1) + d_1, \quad (13)$$

and

$$Z_2(y) = a_2\, erfc(b_2 y + c_2) + d_2. \quad (14)$$

However, a strong stress on the oxide grown underneath a thick nitride mask results in a 'pinch' of oxide near the mask edge. In this case, following functions are used to simulate 'bird's beak' on the two sides of the 'pinch' (Guillemot *et al* 1987b).

$$Z_1(y) = a_1'\, erfc(b_1'(y - \delta)), \quad \text{for } y \geq \delta, \quad (15)$$

$$Z_1(y) = e'_1 \frac{d_1' - y}{d_1' - y + q}, \quad \text{for } y \leq \delta, \quad (16)$$

$$Z_2(y) = a_2'\, erfc(b_2' y) + c_2', \quad \text{for } y \geq 0, \quad (17)$$

$$Z_2(y) = e_2' \frac{d_2' - y}{d_2' - y + q}, \quad \text{for } y \leq 0, \quad (18)$$

where $q = 0{\cdot}05\ \mu m$ and $\delta = 0{\cdot}04\ \mu m$. The parameters a_1, b_1, c_1, d_1 ... etc are related to parameters like oxide thickness (e_{ox}), mask thickness (e_n), thickness of oxide grown (E_{ox}) (simulated by Deal and Grove's (1965) Model), extant of bird's beak under the mask (L_{bb}) and silicon nitride mask lifting parameter (H). The boundary conditions are: $z_1(y) = z_2(y) = 0$ for y values ≤ 0 or ≥ 0 except $z_2(y) = -e_{ox}$ for $y \geq 0$. The other details can be seen from the article of Guillemot *et al* (1987b).

4. Algorithm for 2D-partial differential equation solver

Finite difference and finite element approaches have been followed to solve diffusion equations [i.e. (1), (2) or (9)] numerically in the literature. The earlier simulators (Penumalli 1983; Maldoado *et al* 1983; Lorenz *et al* 1985; Kump and Dutton 1988; Nishi *et al* 1989; Rorris *et al* 1990; Fair *et al* 1991) were based on the PDE solution by finite difference method (FDM). On the other hand, the second generation simulators (Borucki *et al* 1985; O'Brien *et al* 1985; Collard and Taniguchi 1986) were built on finite element method (FEM) due to the ease of handling moving boundary problems in FEM. However, the finite element approach is complex, and requires high computational resources. In the finite difference scheme, both implicit and explicit methods have been successfully used for the numerical solution of diffusion problems. In terms of operations per time step, implicit scheme is more CPU time intensive than explicit methods but it allows larger time steps and is unconditionally stable compared to the latter in which most schemes have conditional dependence (Lapidus and

Pinder 1982). The stability, simplicity of code and less stringent hardware requirements motivated us to adopt FDM based on implicit scheme to solve the present problem. Moreover, with the advent of vector machines, this scheme is also advantageous as compared to finite element scheme since it results in more ordered data structure suitable for vectorization and parallelization, although a solver based on explicit method was used to compare results (Singh and Das 1998).

For two-dimensional simulation of impurity and oxidation profiles a small portion of device is chosen such that the impurity concentration gradient is zero at its edges (to satisfy the boundary conditions). It is referred to as 'domain' in the present text and is shown in figure 1. An efficient algorithm for non-uniform mesh generation was developed wherein the user can define a number of regions (in normal and lateral directions) in the 'domain' and within these regions non-uniform grids can be set. This increases simulation accuracy and decreases computational requirement in terms of resources and time. As the simulation 'domain' has a fixed number of rectangular elements, the total number of mesh points in all the regions should not exceed the physical array dimensions. It enables the user to generate non-linear grids and consequently, to have finer grids in the region where doping concentration varies sharply with distance and to have coarse grids in the region where the change is not so pronounced without sacrificing the accuracy. Once the initial grid has been set-up it is adjusted as various process steps are simulated. The complete diffusion equations were discretized at mid points between nodes (Singh 1997). An iterative method known as 'line by line method' which sets up a pseudo-tridiagonal matrix rather than a penta-diagonal matrix has been used to calculate concentrations (Patanker 1980).

A logic by which the time step is automatically varied

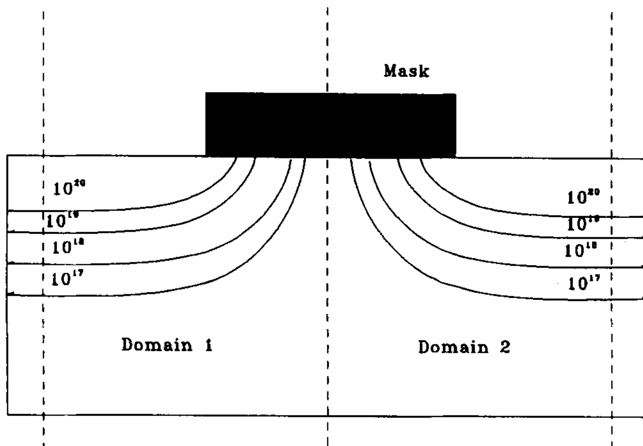

Figure 1. 'Domain', the simulation area bounded by vertical lines on left and right sides (where the concentration gradient is zero in lateral direction) of a device feature.

as the solution proceeds with time to improve computational efficiency without sacrificing accuracy has been developed. It uses the difference between the concentration values determined in current time step (C^n) and the value projected (C^{proj}) with linear fit in previous time steps (C^{n-1} and C^{n-2}) to calculate the projected time step (δt^{proj}) as following (Singh and Das 1987),

$$\delta t^{\text{proj}} = \delta t^n \left(\frac{1 + \dfrac{\delta t^{n-1}}{\delta t^n}}{\max \| \eta \|} \right), \tag{19}$$

where the maximum error η is defined as,

$$\eta = \frac{C^n_{i,j} - C^{\text{proj}}_{i,j}}{\| C^n_{i,j} * \eta_{\text{rel}} + \eta_{\text{abs}} \|}, \tag{20}$$

and the $C^{\text{proj}}_{i,j}$ is defined as,

$$C^{\text{proj}}_{i,j} = C^n_{i,j} + (C^n_{i,j} - C^{n-1}_{i,j}) \frac{\delta t^n}{\delta t^{n-1}}. \tag{21}$$

The default values of absolute (η_{abs}) and relative (η_{rel}) errors are 1×10^{10} and 1×10^{-2}, respectively. In fact, δt^{proj} is the next time step value, δt^{n+1}, provided other processes may not limit it further. Indeed, the value of δt^{n+1} finally accepted is restricted in diffusion module where the minimum of the values returned by the individual process steps and the projected time is taken. It has been observed that a highly non-uniform time step as large as 20–30 times of the minimum time step (dt^{min}) generally resulted in a single process simulation as can be seen from figure 2. This led to high computational efficiency of the program.

It is often desirable in iterative solutions of the non-linear algebraic equations to speed up or slow down the changes, from one iteration to another. Successive relaxation criteria has been built-in in "2D-DIFFUSE" as given below (Patanker 1980),

$$C^{\text{itr}}_{i,j} = \alpha^{\text{sor}} C^{\text{itr}}_{i,j} + (1 - \alpha^{\text{sor}}) C^{\text{itr}-1}_{i,j}, \tag{22}$$

where $C^{\text{itr}}_{i,j}$ and $C^{\text{itr}-1}_{i,j}$ are the calculated concentration values at a particular iteration (itr) and an iteration previous to that, respectively and α^{sor} is the relaxation parameter.

Diffusion of dopants, viz. B, P, As and Sb in silicon under neutral and oxidizing ambient based on advanced models has been incorporated for intrinsic and extrinsic diffusion. Process related effects such as band gap narrowing (BGN) after heavy doping, oxidation enhanced (OED) and retarded diffusion (ORD), has been taken care off (Singh and Das 1987).

In order to calculate diffusion during oxidation and OED/ORD, fluxes at moving silicon–oxide interface are

to be determined. This has been done by mapping the simulated 'Bird's Beak' on the non-linear grids. The mapped shape was digitized such that the interface remains either parallel to the grid lines or crosses a cell diagonally and then fluxes were calculated. After this the oxide interface was allowed to move further downward inside silicon in subsequent time steps and mesh regridding was done. This sequence was repeated at each time step till the process was over (Singh *et al* 1996; Singh and Das 1998).

A software for visual display in terms of one- and two-dimensional profiles of the data has been built-in along with the process simulator. The 2D diffusion profiles given in this paper have been plotted using this program. '2D-DIFFUSE' is based on modular structure. The portability of the program on DOS and UNIX OS has been ensured. The input such as grid and process parameters can be set interactively in '2D-DIFFUSE'. All these features make the program user-friendly.

5. Results and discussion

In IC technology various process steps involve a high temperature processing of the wafer under different surface and ambient conditions. A newer process of thermal nitridation of silicon and silicon dioxide, which appears to be an alternative to the thin oxide that has both technological and reliability problem, is one example of a different surface condition. Another such example is annealing subsequent to deposition of metal silicides which are used to make ohmic contacts, gates and interconnect lines in IC technology. All these process conditions perturb the point defects concentration and their distribution in the wafer either by injecting vacancies or interstitials and consequently affect diffusion of impurities (Hayafugi *et al* 1982; Fahey *et al* 1983, 1985, 1989; Wittmer and Tu 1984; Moslehi and Saraswat 1985; Hu 1987; Wen *et al* 1987; Ahn *et al* 1988a, b; Fahey and Dutton 1988; Mogi *et al* 1996; Herner *et al* 1996, 1997). The old concept of vacancy assisted diffusion (Fair 1981) was only able to explain why the diffusion of boron and phosphorus is enhanced and that of antimony is retarded during oxidation. On the other hand, the observed phenomenon like retarded diffusion of antimony and enhanced diffusion in case of phosphorus and boron under nitridation could not be explained on the basis of single species diffusion model. This led to the development of dual defects based models. It has now been well established that the diffusion of substitutional dopant in silicon are mediated both by vacancies and self-interstitials and which accounts for most non-equilibrium effects seen in diffusion.

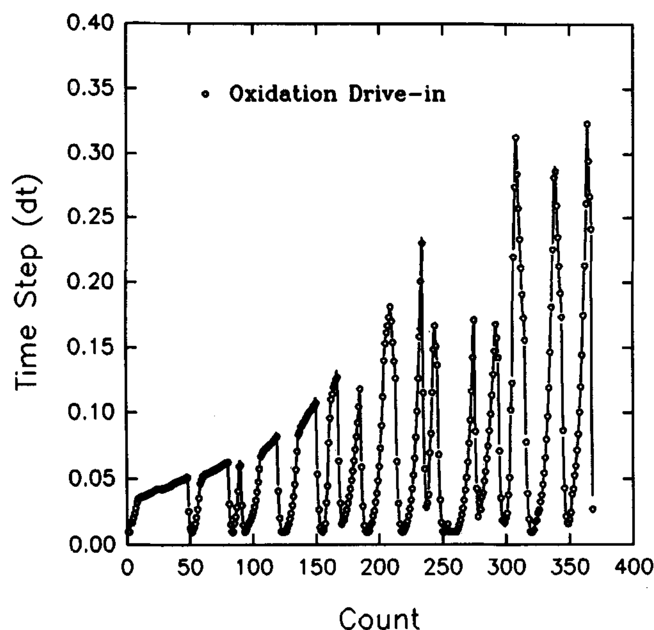

Figure 2. Variation of time step with count (in terms of process duration) showing the non-uniform time step, 'dt' for oxidation process.

Considering the high number of possible species and their reactions, various assumptions are made until proper diffusion equations mentioned in preceding section were obtained. The coupled system of impurity and point defect diffusion equations is stiff numerically due to the difference in the diffusion coefficients of the point defects and dopant impurities which is some times as large as eight orders of magnitude (Leroy 1979; Taniguchi *et al* 1983; Bronner and Plummer 1985, 1987; Tan and Gosele 1985; Griffin and Plummer 1986). Additionally, the wide range of bulk and surface recombination velocities lead to the defects equations to be stiff numerically.

There are two schools of thought about the distribution of point defects. One believes that the quasi steady state reaches in a very short time compared to total processing time (i.e. $\partial C/\partial t = 0$) and the defects distribution is uniform over the impurity simulation domain whereas the other thought is that there exists a transient state. The experimental evidences are in favour of the former.

The diffusion equations of point defects can be solved numerically either in totality or by decoupling the two equations. The procedure for the former involving solution of coupled PDE's is computationally exhaustive. Two approaches have been commonly adopted to decouple the point defect equations (Law and Dutton 1988; Law 1990; Taniguchi *et al* 1990).

(I) If the recombination between interstitials and vacancies is considered to be weak compared to the diffusion and surface recombination and generation assuming that the depleted vacancies are replenished instantaneously from the surface. In this case $C_V = C_V^*$ can be assumed. (II) If the surface is weakly able to replenish the bulk and local equilibrium of point defects exists then $C_I C_V = C_I^* C_V^*$ can be assumed in the bulk. This condition not

only serves the purpose of decoupling the two point defect equations but also allows analytical solution of the problem under quasi steady state.

These two simplifying conditions are referred to as vacancy equilibrium and quasi-equilibrium conditions, respectively in the subsequent text. In the present study both the conditions have been applied to determine the excess interstitials concentration profiles.

The major difficulty faced during early stages of point defect based computer modelling by software engineers and which exists still up to some extent is the inconsistency in various parameter values. Some times the disagreement is as large as several orders of magnitude. For example, the diffusion coefficients of interstitials from various sources (Leroy 1979; Taniguchi *et al* 1983; Bronner and Plummer 1985, 1987; Griffin and Plummer 1986) are three to four orders of magnitude different as can be seen from figure 3. This makes the choice of numerical algorithm more difficult as its suitability depends heavily on the magnitude of these parameters specially the diffusion coefficients of the various species.

All the point defect parameters are difficult to extract from experiments since they can not be measured directly. Oxidation enhanced diffusion, the most widely studied phenomenon, is used to understand point defect transport and their recombination. These studies were the basis of point defect modelling and were used to deduce diffusion coefficients and equilibrium concentrations of point defects and other parameters. However, inconsistency among the parameters from different sources has been the major concern. In order to overcome this problem some workers have adopted an indirect method to have information about other defect parameters. For example, Law (1990) has extracted various point defect parameters from best fit of the simulation and experimental data by using the data of the parameters which can be determined experimentally accurately. The two sets of parameter values listed in table 1 are deduced from D_{I} and C_{I}^{*} values after Bronner and Plummer (1987) and Boit *et al* (1990) by Law (1990) using SUPREM-IV. The SUPREM-IV default values (Law *et al* 1986; TSUPREM 1992) of these parameters are also listed in table 1 for comparison.

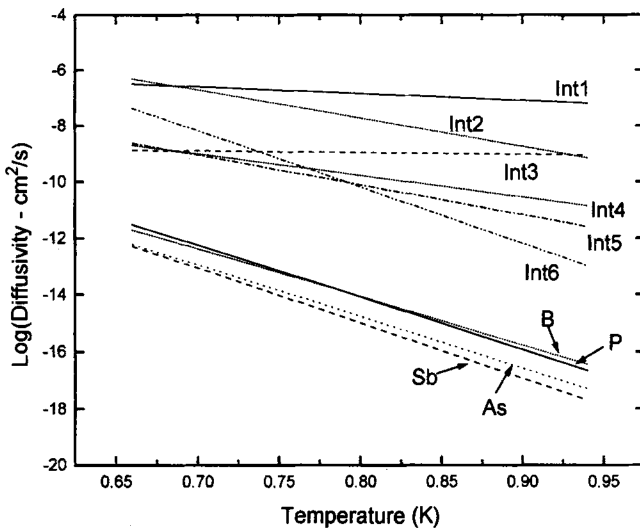

Figure 3. Diffusion coefficients of interstitials from different sources (Int1: Tan and Gosele 1985; Int2: Leroy 1979; Int3: Bronner and Plummer 1985; Int4: Kump and Dutton 1988; Int5: Griffin and Plummer 1986; Int6: Taniguchi *et al* 1983) and of the common dopant impurities (B, P, As and Sb: Fair 1981) as a function of temperature.

The large difference observed in interstitial diffusivity from various sources has been attributed to the existence of the interstitial traps (Griffin and Plummer 1986) which are assumed to be dependent on history of substrate (FZ, CZ, epitaxial etc) and the prior processing (e.g. gettering etc) conditions.

The vertical and lateral defect profiles are strongly anisotropic. This is because the interstitials decay length is different in the two directions and is much shorter in the latter (OED measured under pad oxide). Shorter decay length is caused by the combination of three mechanisms in the lateral direction: bulk recombination with vacancies, bulk recombination with traps and surface recombination along the silicon–silicon dioxide interface.

In order to see the performance and limitations of '2D-DIFFUSE' and to make it bug free, a number of simulations for different input parameters viz. temperature, time, ambient, etc were carried out. Some of the simulated results have been shown here.

Figures 4 and 5 show typical two-dimensional interstitial and vacancy profiles, respectively for very short oxidation. A short duration of oxidation gave point defect profiles in the region depicted in the figures. For large oxidation time, the entire simulation domain will have high interstitials concentration and low vacancy concentrations which are difficult to plot. Interstitial concentration decreases from its maximum value at the interface to its minimum (i.e. equilibrium) value with the increase in the depth in normal direction. An opposite behaviour is observed in the case vacancies. The interstitial profiles in normal direction (i.e. along the depth of the wafer) are depicted in figure 6 where qualitative profiles are plotted in three regions: at oxidizing surface far away from the mask, at the edge of the mask and deep inside the mask. The interstitial concentration in the region far away from the masked region, decreases with the depth monotonically. On the other hand, the interstitial concentrations both at the edge of the mask and under the mask region, increase initially and show distinct peaks which fade away as one moves away from the masked region in the lateral direction. The interstitial concentra-

tion profiles match with the equilibrium value far away from the surface in the normal direction. The curves show highly anisotropic behaviour of the lateral diffusion and demonstrate the effectiveness of the surface recombination under the mask as defined by the boundary condition ((4) and (5)). Just an opposite behaviour has been observed in the case of vacancies profile which has also been plotted in figure 6 corresponding to the interstitial concentration under the mask edge for the sake of comparison.

Figure 7 shows interstitial concentration as a function of depth for various times during the wet oxidation step using quasi equilibrium model. This figure illustrates the strong time dependence of interstitials specially for short process durations. Figure 8 depicts interstitial and vacancy profiles for a longer (25 min at 950°C) wet oxidation process.

A number of simulations for drive-in under oxidizing ambient have been carried out in order to see the effect of point defects on impurity diffusion. For the sake of

Table 1. Values of point defect parameters.

	Bronner and Plummer (1987)		Boit *et al* (1990)		SUPREM-IV (TSUPREM 1992)	
Parameter	Preexponential term	Activation energy	Preexponential term	Activation energy	Preexponential term	Activation energy
D_I	$600{\cdot}0$ cm^2/s	2·44 eV	$1{\cdot}03\times10^2$ cm^2/s	3·22 eV	$3{\cdot}65\times10^{-4}$ cm^2/s	1·58 eV
C_I^*	$5{\cdot}0\times10^{22}$ cm^{-3}	2·36 eV	$3{\cdot}11\times10^{19}$ cm^{-3}	1·58 eV	$1{\cdot}25\times10^{29}$ cm^3	3·26 eV
D_V	$0{\cdot}10$ cm^2/s	2·00 eV	$6{\cdot}34\times10^3$ cm^2/s	3·29 eV	$3{\cdot}65\times10^{-4}$ cm^2/s	1·58 eV
C_V^*	$2{\cdot}0\times10^{-23}$ cm^{-3}	2·0 eV	$4{\cdot}77\times10^{18}$ cm^{-3}	0·713 eV	$1{\cdot}25\times10^{29}$ cm^3	3·26 eV
$K_{I\min}$	$2{\cdot}89\times10^{-2}$ cm/s	0·834 eV	$1{\cdot}204\times10^{-3}$ cm/s	0·44 eV	$6{\cdot}01\times10^{-13}$ cm/s	− 1·58 eV
$K_{I\max}$	$1{\cdot}29\times10^5$ cm/s	1·77 eV	$8{\cdot}18\times10^5$ cm/s	1·95 eV	$6{\cdot}01\times10^{-13}$ cm/s	− 1·58 eV
α_I	3·99	0·228 eV	0·91	0·051 eV	0·0	0·0
Θ	54·7	0·889 eV	1·97	0·55 eV	0·01	0·0
$K_{V\min}$	$1{\cdot}37\times10^3$ cm/s	2·19 eV	$1{\cdot}12\times10^4$ cm/s	2·48 eV	$6{\cdot}01\times10^{-15}$ cm/s	− 1·58 eV
$K_{V\max}$	$1{\cdot}91\times10^9$ cm/s	3·40 eV	$2{\cdot}93\times10^{16}$ cm/s	5·36 eV	$6{\cdot}01\times10^{-15}$ cm/s	− 1·58 eV
α_V	$6{\cdot}1\times10^{-2}$	− 0·39 eV	$1{\cdot}79\times10^{-7}$	− 1·91 eV	0·0	0·0
K_R	$7{\cdot}22\times10^{-19}$ cm^3/s	0·96 eV	$1{\cdot}40$ cm^3/s	3·99 eV	0·0	0·0
C_{TOT}	$1{\cdot}0\times10^{18}$ cm^{-3}	0·0 eV	$2{\cdot}0\times10^{18}$ cm^{-3}	0·0 eV	0·0	0·0
C_{ET}^*	$2{\cdot}96\times10^{21}$ cm^{-3}	1·03 eV	$4{\cdot}77\times10^{-23}$ cm^{-3}	1·57 eV	0·0	0·0
K_T	$6{\cdot}39\times10^6$ cm^3/s	2·44 eV	$1{\cdot}10\times10^{21}$ cm^3/s	3·22 eV	0·0	0·0

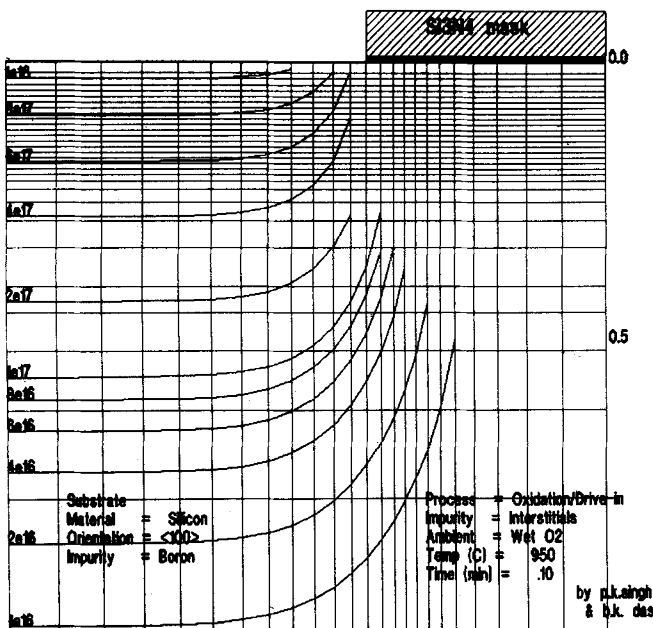

Figure 4. Simulated interstitial equi-concentration contours for 0·1 min at 950°C under wet oxidizing ambient.

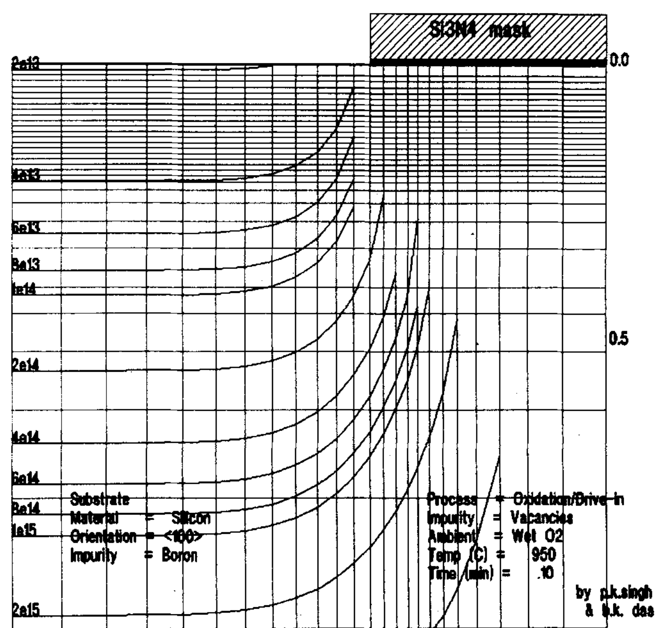

Figure 5. Simulated vacancy equi-concentration contours for 0·1 min at 950°C under wet oxidizing ambient.

comparison between drive-ins under neutral and oxidizing ambients, the input parameters for the pre-deposition and the subsequent oxidation step have been taken exactly the same except for the ambient. Additionally, three sets of results have been simulated by using the set of point defect parameters listed in table 1. In one typical example illustrated here, boron (10^{14} atom/cm^3) pre-doped ⟨100⟩ silicon wafer partially covered with 0·2 μm thick nitride mask with 0·01 μm pad oxide underneath, has been considered for phosphorous pre-deposition at 900°C for 5 min under neutral ambient. The pre deposition has been followed by oxidation in wet ambient at 950°C for 3 min. The simulated results in the form of iso-concentration contours for interstitials, vacancies and impurity (phosphorous) have been shown in figure 9, 10 and 11 for Boit *et al* (1990), Bronner and Plummer (1987) and SUPREM-IV (TSUPREM 1992) data, respectively. Figure 12 illustrates 2D contours for the drive-in carried out under non oxidizing ambient for the same set of parameters. The comparison of figures 9–11 brings out the following facts. Boit *et al* and Bronner and Plummer models simulate practically the same phosphorous profiles. However, the interstitial profile is deeper in the former. On the other hand, the dopant as well as defect profile are much deeper after SUPREM-IV based data both in normal and lateral directions.

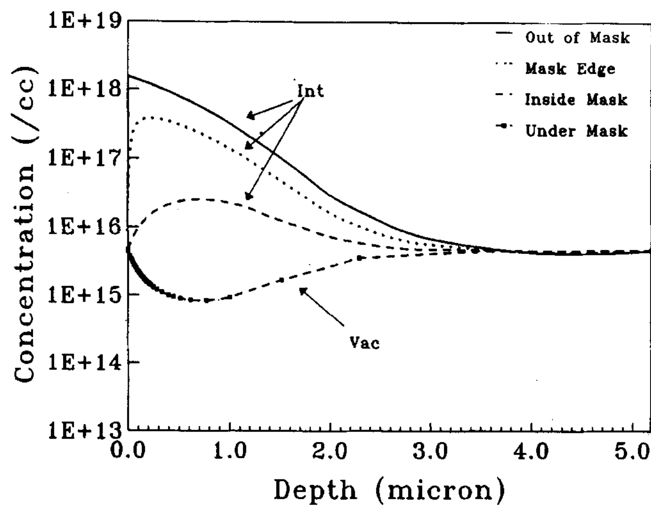

Figure 6. One-dimensional interstitial (Int) profiles along the depth of the wafer at various positions along the top interface, i.e. at the oxidizing interface, at the edge of the mask and under the mask. The vacancy (Vac) profile under the mask corresponds to the interstitial profile at the same position.

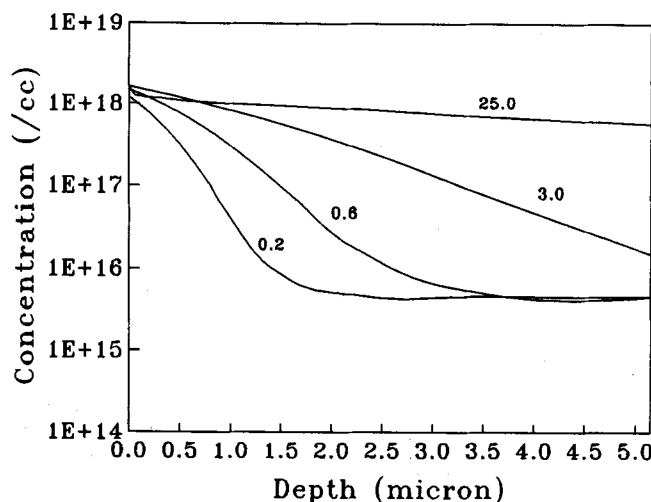

Figure 7. One-dimensional interstitial profiles as a function of depth for various duration of oxidation (0·2, 0·6, 3·0 and 25·0 min).

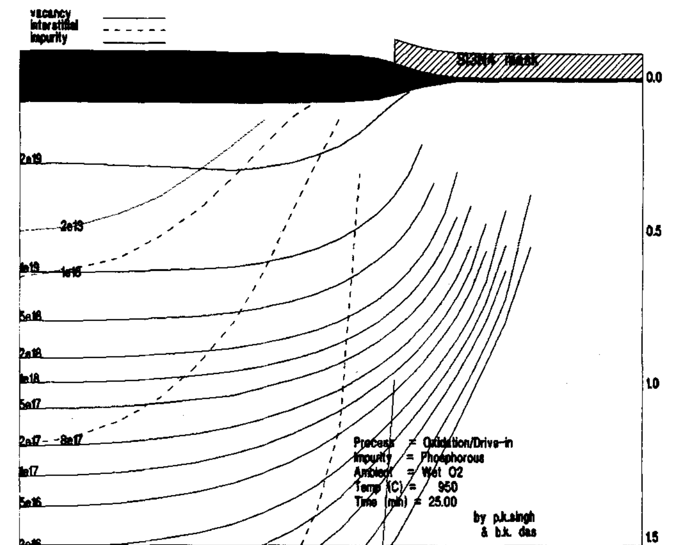

Figure 8. Simulated equi-concentration contours of interstitials, vacancies and phosphorous for 25 min at 950°C under wet oxidizing ambient.

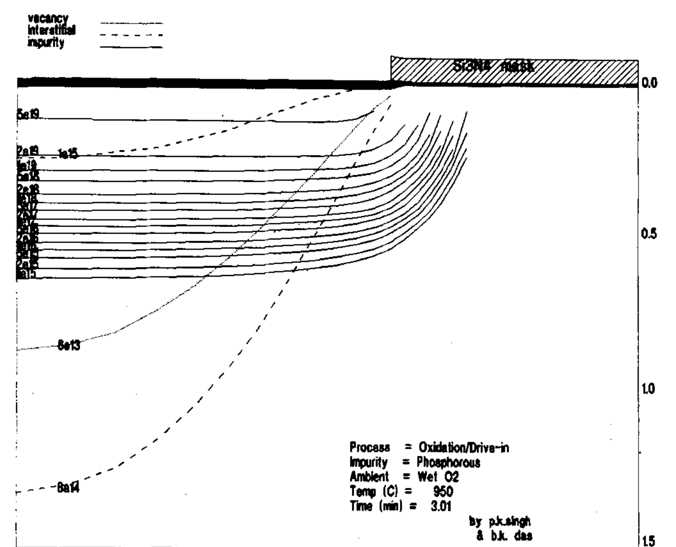

Figure 9. Results of '2D-DIFFUSE' simulation showing phosphorous iso-concentration contours after drive in for 3 min at 950°C under oxidizing ambient (using Boit *et al* (1990) parameters for point defect).

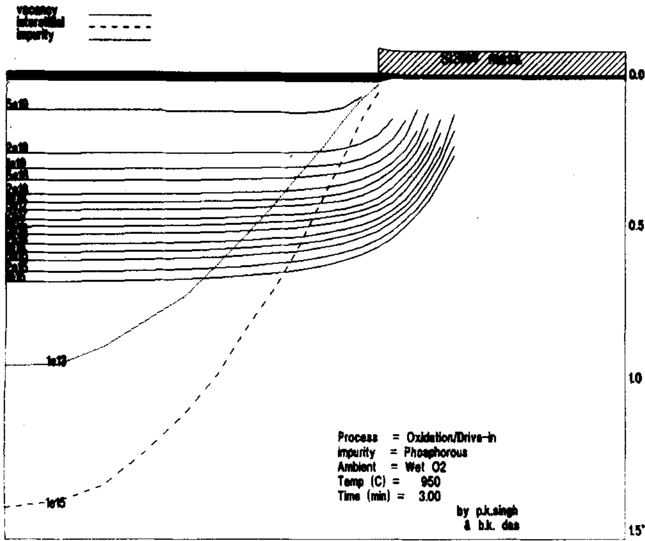

Figure 10. Results of '2D-DIFFUSE' simulation showing phosphorous iso-concentration contours after drive in for 3 min at 950°C under oxidizing ambient (using Bronner and Plummer (1987) parameters for point defect).

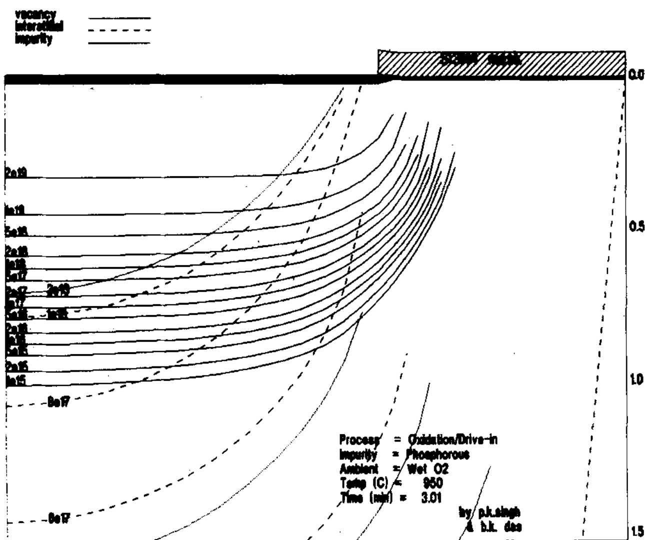

Figure 11. Results of '2D-DIFFUSE' simulation showing phosphorous iso-concentration contours after drive in for 3 min at 950°C under oxidizing ambient (using SUPREM-IV (TSUPREM 1992) parameters for point defect).

The comparisons of figure 12 with figures 9–11 reveal the OED for phosphorous where the dopant has diffused much deeper into the wafer (i.e. in normal direction) as well as under the mask edge (i.e. in lateral direction) after oxidation in comparison to neutral conditions for all the three sets of data. However, OED effect is more pronounced after SUPREM-IV based data. Similar enhanced diffusion has been observed in the case of B and As also whereas retarded diffusion has been observed in the case of Sb.

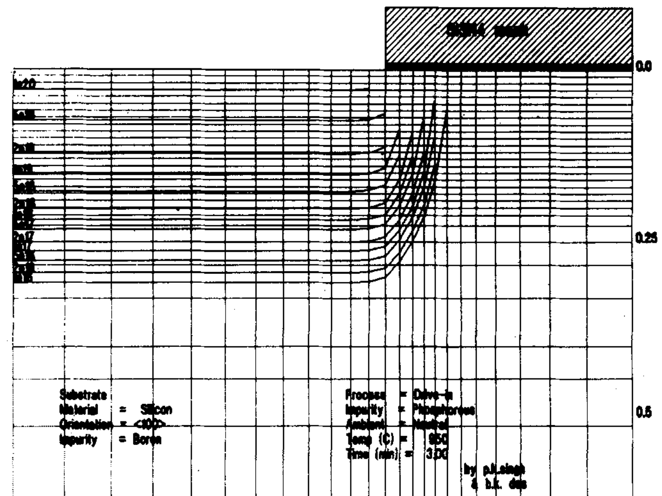

Figure 12. Results of '2D-DIFFUSE' simulation showing phosphorous iso-concentration contours after drive in for 3 min at 950°C under neutral ambient.

Another set of simulation has been carried out using the two decoupling assumptions discussed above to bring out the difference in the point defect profiles and their effect on impurity diffusion. The quasi steady state assumption provided shallower interstitial profile in comparison to the constant vacancy concentration assumption.

6. Conclusion

This paper describes a two-dimensional process simulator which uses finite difference method to solve coupled diffusion equation of point defects and dopants. The spatial discretization by finite difference and an iterative 'line by line' method which sets up a pseudo tridiagonal matrix have shown to be well suited for the solution of coupled defect–dopant coupled diffusion problem. The process simulator was applied successfully to the simulation of such phenomena as the dopant diffusion under various ambients, oxidation enhanced and retarded diffusion etc.

Acknowledgement

The authors are thankful to Dr S N Singh for discussion.

References

Ahn S T, Kennel H W, Plummer J D and Tiller W A 1988a *Appl. Phys. Lett.* **53** 1593

Ahn S T, Kennel H W, Plummer J D and Tiller W A 1988b *J. Appl. Phys.* **64** 4914

Antoniadis D A and Dutton R W 1979 *IEEE Trans. Electron Devices* **ED-26** 490

Atalla M M and Tannenbaum E 1960 *Bell System Tech. J.* **39** 933

Boit C, Lau F and Sittig R 1990 *Appl. Phys.* **A50** 197
Borucki L, Hansen H H and Varahramyan K 1985 *IBM J. Res. & Dev.* **29** 263
Bronner G B and Plummer J D 1985 *Impurity diffusion and gettering in silicon* (eds) R B Fair and C W Pearce (*Proceedings MRS*) (New York: North Holland) Vol. 36 p. 36
Bronner G B and Plummer J D 1987 *J. Appl. Phys.* **61** 5286
Chin D, Kump M and Dutton R W 1981 *SUPRA – Stanford University Process Simulation Program* (Stanford University Report 1981)
Chin D, Oh S Y, Hu S M, Dutton R W and Moll J L 1983a *IEEE Trans. Electron Devices* **ED-30** 744
Chin D, Oh S Y and Dutton R W 1983b *IEEE Trans. Electron Devices* **ED-30** 993
Collard D and Taniguchi K 1986 *IEEE Trans. Electron Devices* **ED-33** 1454
Deal B E and Grove A S 1965 *Appl. Phys. Lett.* **36** 3770
DoE 1993 Manual for 1D-STEPS (Department of Electronics, Government of India, Delhi)
Fair R B 1981 *Impurity doping processes in silicon* (ed.) F F Y Wang (New York: North Holland)
Fair R B 1988 *IEEE Trans. Electron Devices* **ED-35** 285
Fair R B, Gardner C L, Johnson M J, Kenkel S W, Rose D J, Rose J E and Subrahmanyan R 1991 *IEEE Trans. Computer Aided Design* **CAD-10** 643
Fahey P and Dutton R W 1988 *Appl. Phys. Lett.* **52** 1092
Fahey P, Dutton R W and Moslehi 1983 *Appl. Phys. Lett.* **43** 683
Fahey P, Barbuscia G, Moslehi and Dutton R W 1985 *Appl. Phys. Lett.* **46** 784
Fahey P, Iyer S S and Scilla G J 1989 *Appl. Phys. Lett.* **54** 843
Griffin P B and Plummer J D 1986 *Technical digest of international IEDM meeting, Los Angeles, USA* p. 522
Grove A S, Leistiko O and Sah C T 1964 *Appl. Phys. Lett.* **35** 2695
Guillemot N, Pananakakis G and Chenvier P 1987a *IEEE Trans. Electron Device* **ED-34** 1033
Guillemot N, Pananakakis G and Chenvier P 1987b *Revue Phys. Appl.* **22** 477
Hayafugi Y, Kajiwara K and Usui S 1982 *J. Appl. Phys.* **53** 8639
Herner S B, Jones K S, Gossmann H-J, Tung R T, Poate J M and Luftman H S 1996 *Appl. Phys. Lett.* **68** 2870
Herner S B, Jones K S, Gossmann H-J, Tung R T, Poate J M and Luftman H S 1997 *J. Appl. Phys.* **82** 583
Ho C P, Plummer J D, Hansen S E and Dutton R W 1983 *IEEE Trans. Electron Devices* **ED-30** 1438
Hu S M 1974 *J. Appl. Phys.* **45** 1567
Hu S M 1983 *Appl. Phys. Lett.* **43** 449
Hu S M 1985 *J. Appl. Phys.* **57** 1069
Hu S M 1987 *Appl. Phys. Lett.* **51** 308
Hu S M and Schmidt S 1968 *Appl. Phys. Lett.* **39** 4272
Kump M R 1988 *Two-dimensional computer simulation of diffusion in silicon*, Doctoral Dissertation, Stanford University, Stanford, USA
Kump M R and Dutton R W 1988 *IEEE Trans. Computer Aided Design* **CAD-7** 191
Lapidus P and Pinder G F 1982 *Numerical solution of partial differential equations in science and engineering* (New York: Wiley)
Law M E 1990 *IEEE Trans. Computer Aided Design* **CAD-9** 1125
Law M E and Dutton R W 1988 *IEEE Trans. Computer Aided Design* **CAD-7** 181
Law M E, Rafferty C and Dutton R W 1986 *SUPREM-IV User's Manual* (USA: Stanford University)
Lee H-G 1978 TR No G-201-8, Stanford University Microelectronics Laboratories (Stanford University)
Lehovec K and Slobodskoy A 1961 *Solid State Electron.* **3** 45
Leroy B 1979 *J. Appl. Phys.* **50** 7996
Lin A M, Dutton R W, Antoniadis D A and Tiller W A 1981 *J. Electrochem. Soc.* **128** 1121
Lindhard J, Schraff M and Schiott M 1963 *Mat. Fys. Medd. Dan. Vid. Sclsk* **33** 1
Lorenz J, Pelka J, Ryssel H, Sachs A, Seidl A and Svoboda M 1985 *IEEE Trans. Electron Devices* **ED-32** 1977; *IEEE Trans. Computer Aided Design* **CAD-4** 421
Maldoado C D, Custode F Z, Louie S A and Pancholy R K 1983 *IEEE Trans. Electron Devices* **ED-30** 1462
Mogi T K, Thompson M O, Gossmann H-J, Poate J M and Luftman H S 1996 *Appl. Phys. Lett.* **69** 1273
Moslehi M M and Saraswat K C 1985 *IEEE Trans. Electron Devices* **ED-32** 106
Mulvaney B J, Richardson W B and Crandle T L 1989 *IEEE Trans. Computer Aided Design* **CAD-8** 336
Nishi K, Sakamoto K, Kuroda S, Ueda J, Miyoshi T and Ushio S 1989 *IEEE Trans. Computer Aided Design* **CAD-8** 23
O'Brien R R, Hsieh C M, Moore J S, Lever R F, Murley P C, Brannon K W, Srinivasan G R and Knepper R W 1985 *IBM J. Res. & Dev.* **29** 229
Patanker S V 1980 *Numerical heat transfer and fluid flow* (New York: Hemisphere Pub. Corp.).
Penumalli B R 1983 *IEEE Trans. Electron Devices* **ED-30** 986
Rorris E, O'Brien R R, Morehead F F, Lever R F, Peng J P and Srinivasan G R 1990 *IEEE Trans. Computer Aided Design* **CAD-9** 1113
Ryssel H, Haberger K, Hoffmann K, Prinke G, Dumcke R and Sachs A 1980 *IEEE Trans. Electron Devices* **ED-27** 1484
Seidl A 1983 *IEEE Trans. Electron Devices* **ED-30** 722
Sakamoto K, Nishi K, Yamaji T, Miyoshi T and Ushio S 1985 *J. Electrochem. Soc.* **132** 2457
Singh P K 1997 *DoE Project Report* (unpublished)
Singh P K and Das B K 1997 unpublished
Singh P K and Das B K 1998 *Physics of semiconductor devices* (ed.) V Kumar and S K Agrawal (New Delhi: Narosa Publication) p. 1060
Singh P K, Saha S, Singh A K, Singh S N and Das B K 1996 in *Semiconductor devices* (ed.) K Lal (New Delhi: Narosa Publishing House) p. 277
Tan T Y and Gosele U 1985 *Appl. Phys.* **A-37** 1
Taniguchi K, Antoniadis D A and Matsushita Y 1983 *Appl. Phys. Lett.* **42** 1983
Taniguchi K, Shibata Y and Hamaguchi C 1990 *IEEE Trans. Computer Aided Design* **CAD-9** 1177
TSUPREM-IV 1992 *Users manual* (USA: TMA Corporation)
Wen D S, Smith P L, Osburn C M and Rozgonyi G A 1987 *Appl. Phys. Lett.* **51** 1182
Wittmer M and Tu K N 1984 *Phys. Rev.* **B29** 2010
Wolf S 1990 in *Silicon processing for the VLSI era* (Sunset Beach, USA: Lattice Press)